Experimental Study of a Three-Phase Diode Rectifier Operating at Cryogenic Temperature

Yasmine Baazizi, Lauro Ferreira, Simon Meunier, Tanguy Phulpin, Loïc Quéval

Experimental study of a three-phase diode rectifier operating at cryogenic temperature

Yasmine Baazizi, Lauro Ferreira, Simon Meunier, Tanguy Phulpin, Loïc Quéval

***Abstract* — We investigate here the feasibility of operating a three-phase diode rectifier at cryogenic temperature. To do so, several power diodes are tested at room and LN2 temperatures. Then a 3.4 kW three-phase diode rectifier prototype is built and tested at room and LN2 temperatures. Besides we prove that one can predict the performances of such cryogenic diode rectifier by using only the measured diode I-V characteristics. Finally, we assess the relevance of this technology by comparing a cryogenic diode rectifier with its conventional counterpart. The gain may not be in terms of efficiency if cooling power has to be generated, but in terms of power density, since the heat sink is greatly reduced when considering LN2 operation. This study is of interest for compact and lightweight superconducting conversion chains in various sectors, including wind energy and air transportation.**

***Index Terms* — Power electronics, cryogenics, diode rectifier, energy efficiency**

I. INTRODUCTION

Compact, lightweight superconducting conversion chains can significantly reduce the carbon footprint of critical sectors. This is the case in wind power generation, with projects such as EcoSwing [1], SupraPower [2] and EolSupra20 [3], which have highlighted the potential benefits of superconductivity. Or air transport, with initiatives like Airbus/Rolls Royce E-Thrust [4], Nasa N3-X [5], and Airbus ASCEND [6], that have proposed innovative solutions for aircraft electrification. The advantage of using superconductivity is often not justified by a potential gain in efficiency of the machine alone, since large resistive machines are already 98% efficient. Rather, the gain is at the system level, with a reduction in cost, weight or overall volume.

Superconducting conversion chains include machines and cables operating at cryogenic temperatures, requiring power electronics converters between the AC components and the DC bus. Traditionally, these converters operate at room temperature, leading to significant heat input at the interface. By merging the advantages of efficient superconducting cables and machines with cryogenic power electronics, the overall system weight, volume and cost could be significantly enhanced [7]. But until now, most of cryogenic power electronics research has been conducted at the component level [8] – [11].

In this paper, we have three objectives: (i) demonstrate the feasibility of operating a diode rectifier at cryogenic temperature, (ii) check whether one can estimate the performance of such converter from the measured diode I-V characteristic, and (iii) study the relevance of such a solution compared to a conventional one.

In Section 2, we report the experimental characterization of different power diodes, both at room temperature and at liquid nitrogen temperature. The aim is to identify a suitable diode for a cryogenic diode rectifier. In Section 3, we describe our cryogenic diode rectifier prototype and present the experimental results. In Section 4, we present the circuit model of the cryogenic diode rectifier and the simulation results in relation with the objective (ii). In Section 5, we compare an optimally sized cryogenic diode rectifier to a conventional one.

II. CHARACTERIZATION OF POWER DIODES AT CRYOGENIC TEMPERATURE

We have tested dozens of power diodes, but for the sake of clarity, we mention here just two with notable behavior. The first one is the BYT60-400 [12], a fast recovery rectifier diode manufactured by SGS-Thomson Microelectronics. It is made of silicon and comes in a DO-5 package. The second diode is the VS-HFA220FA120 [13], an ultra-fast recovery rectifier diode manufactured by Vishay Semiconductors. It is made of silicon too but comes in a SOT-227 package, a module with two separate diodes.

To measure I-V characteristic of a diode, it is connected in series to a high-current DC power supply [14]. The diode current is measured by the supply, and the diode voltage is measured with a Keithley 2182A nanovoltmeter [15]. The measured I-V characteristics are shown in Fig.1 and the diode parameters are summarized in Table I. For the BYT60-400 diode (Fig. 1a), the resistance slightly decreases at cryogenic temperature, but the threshold voltage significantly increases. As a result, this diode's conduction losses increase when used at cryogenic temperature. It is therefore unsuitable for low-temperature operation. For the VS-HFA220FA120 diode (Fig. 1b), both the resistance and the threshold voltage decrease at cryogenic temperature. This means that this diode has lower conduction losses when operating at low temperatures. It is therefore suitable for use at cryogenic temperature and is selected for the construction of the three-phase diode rectifier.

The project benefited from the financial support of the SuperRail project funded by the French government as part of the Plan de Relance and the Programme d'investissements d'avenir. (*Corresponding author: L. Quéval*).

Yasmine Baazizi, Lauro Ferreira, Simon Meunier, Tanguy Phulpin, and Loïc Quéval are with Université Paris-Saclay, CentraleSupélec, CNRS, GeePs, 91192 Gif-sur-Yvette, France, and with Sorbonne Université, CNRS, GeePs, 75252 Paris, France (e-mail: loic.queval@centralesupelec.fr).

TABLE I
MEASURED DIODE PARAMETERS

Symbol	Parameter	Temp.	BYT60-400	VS-HFA 220FA120
R_{on}	On-state resistance	77 K	8.60 mΩ	2.67 mΩ
		293 K	10.27 mΩ	14.40 mΩ
V_{t0}	Threshold voltage	77 K	1.11 V	1.15 V
		293 K	0.83 V	1.54 V

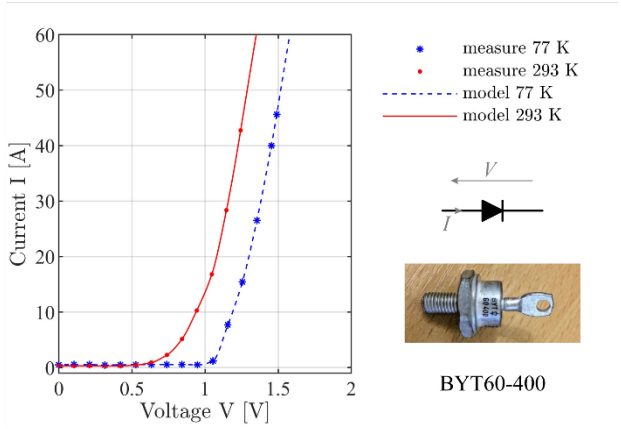

(a) BYT60-400

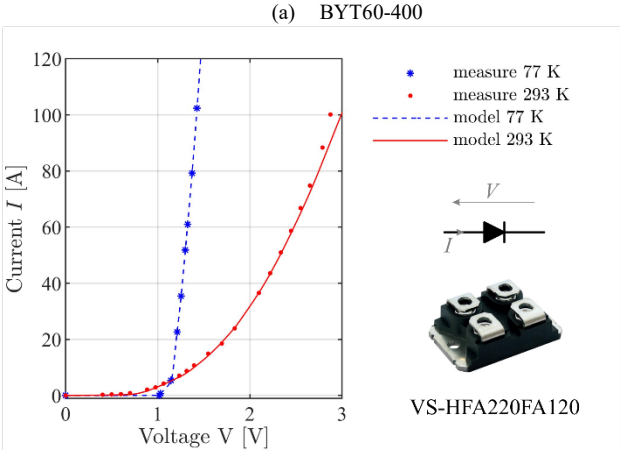

(b) VS-HFA220FA120

Fig. 1. Measured diode current-voltage characteristic.

III. CRYOGENIC DIODE RECTIFIER PROTOTYPE

We designed a three-phase diode rectifier with the following requirements: a nominal AC voltage of 50 V L-L RMS, a nominal frequency of 50 Hz and a nominal power of 3.4 kW. For operation at room temperature (Fig 2a), a 200×300×83 mm anodized aluminum heatsink is selected. Beryllium foil and thermal paste are used to reduce thermal resistance, while providing electrical insulation between the packaging and the heatsink. Note that, for this prototype, the heat sink is oversized.

The same converter is then operated at cryogenic temperature, by cooling it to 77 K in an open liquid nitrogen bath (Fig 2b). The same heat sink is kept for the sake of simplicity, but it would be possible to greatly reduce its size, as will be discussed in section V.

Current is measured with a current probe Tektronix A622 [16], and voltage is measured with a differential voltage probe ST1000 [17]. Both measurements are recorded by a PicoScope 4444 [18]. The voltages are measured as close as possible to the diodes both at the input and at the output.

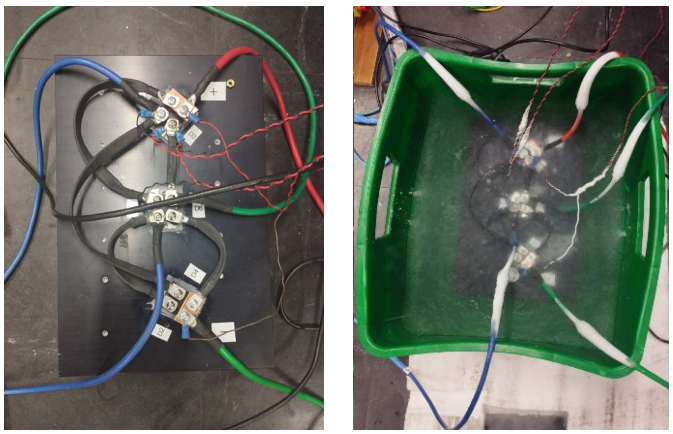

(a) at room temperature (b) at cryogenic temperature

Fig. 2. Diode rectifier prototype.

Fig. 3 and Fig. 4 show the measured AC and DC voltages and currents, for a DC power P_{dc} of 3.4 kW at 77 K. This demonstrates that the rectifier operates as expected. Figures 5 and 6 show the measured diode rectifier losses P_D and efficiency η as a function of the DC power P_{dc}, both at room and cryogenic temperatures. For a DC power P_{dc} of 3.4 kW, the losses at room temperature are 112 W, while at cryogenic temperature they are 80 W. Operating the rectifier at 77 K instead of room temperature thus decreases the losses by 28% and improves efficiency by 1%.

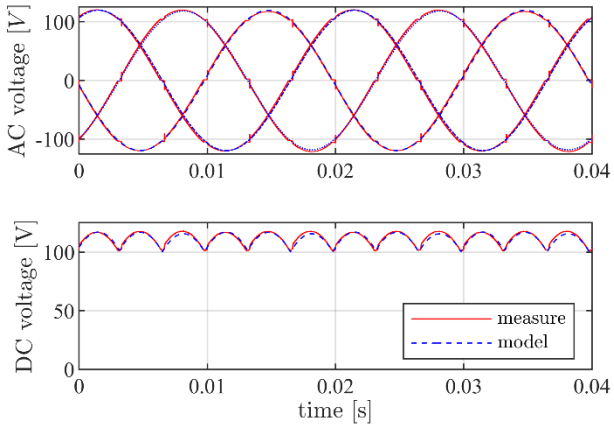

Fig. 3. Measured and simulated diode rectifier AC and DC voltage for 3.4 kW at 77 K.

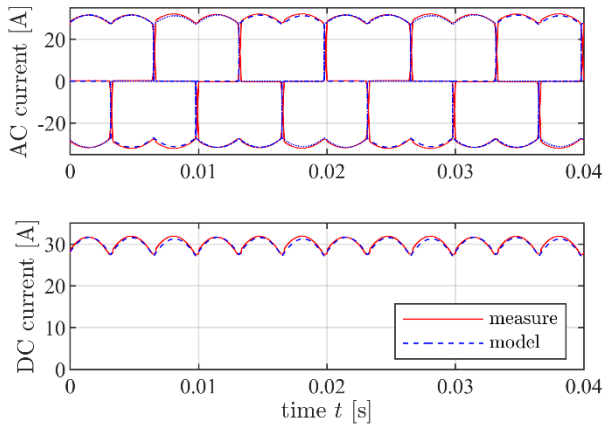

Fig. 4. Measured and simulated diode rectifier AC and DC currents for 3.4 kW at 77 K.

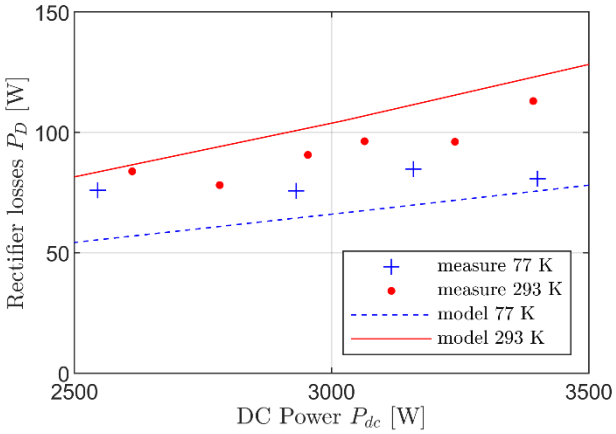

Fig. 5. Measured and simulated diode rectifier losses.

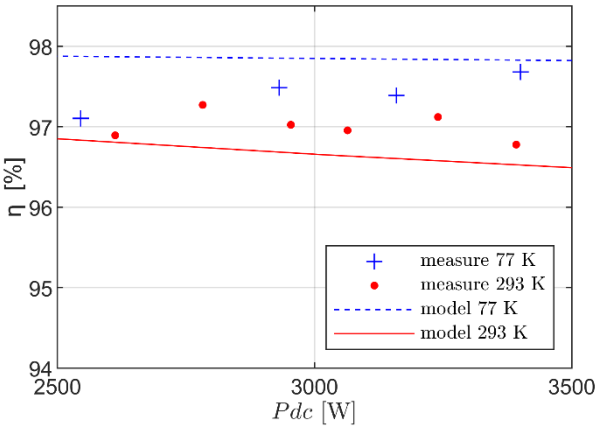

Fig. 6. Measured and simulated diode rectifier efficiency η.

IV. Cryogenic Diode Rectifier Model

In this section, we assess the possibility of estimating the performances of a cryogenic diode rectifier using only the measured I-V characteristic of the diode. To do so, we simulate the converter with a circuit model implemented with the Matlab Simulink Simscape toolbox. The diode is modeled using the "Diode" block, which uses the tabulated I-V characteristic of the diode [19]. This characteristic is derived from 10 experimental data points considering a junction temperature of 293 K for room temperature and 77 K for cryogenic temperature. Such diode model provides an accurate representation of the behavior of the diode (see Fig. 1) while avoiding the need to identify the diode parameters as a function of the temperature. The results of the simulation have been added to Figures 3, 4, 5 and 6. There is a good correspondence between the measure and the model in terms of voltage and current. But the match is only fair for the converter losses and efficiency. This difference may be attributed to various practical factors. Besides, we underline that, while our model takes conduction losses into account, it does not consider switching losses, which are usually negligible at 50 Hz [20], [21]. Overall, the difference between measure and model is deemed acceptable highlighting that using the I-V characteristic of the diode still allows to predict relatively accurately the performance of a cryogenic diode rectifier.

V. Relevance of Cryogenic Converters

In this section, we study the relevance of cryogenic converters compared to conventional ones. This is done by comparing the two systems shown in Fig. 7. Both systems feed a DC load operating at LN2 temperature, such as a superconducting magnet. In topology #T1 (Fig. 7a), the diode rectifier operates at room temperature and is directly connected to the AC source. The load is placed inside the cryostat and is connected to the DC side of the diode rectifier through two DC current leads. In topology #T2 (Fig. 7b), the diode rectifier operates at LN2 temperature and is connected to the AC source through three AC current leads. The load is placed inside the cryostat and is directly connected to the DC side of the diode rectifier. To fairly compare the two solutions, we need to size their heatsink, the current leads and select a suitable cooling option.

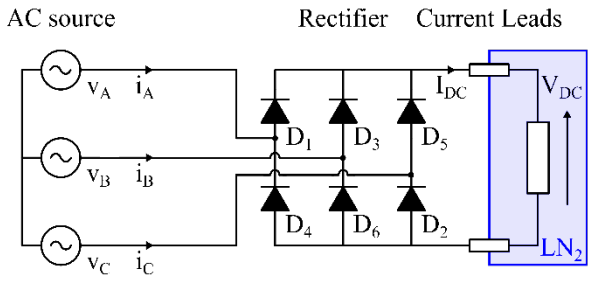

(a) Topology #T1

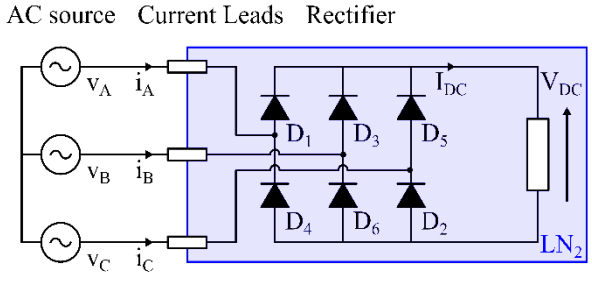

(b) Topology #T2

Fig. 7. Power supply system topologies.

A. Heatsink sizing

The lumped parameter thermal model is solved analytically to obtain the difference between the diode junction temperature T_J and the ambient temperature T_A:

$$T_J - T_A = (R_{JC} + R_{CH} + R_{HA})\, P_D \qquad (1)$$

where R_{JC} is the equivalent junction-case conduction thermal resistance [K/W], R_{CH} is the equivalent case-heatsink conduction thermal resistance [K/W], and R_{HA} is the equivalent heatsink-ambient convection thermal resistance [K/W]. Sizing the heatsink involves selecting its reference and dimension. This corresponds to selecting R_{HA} so that T_J remains below the maximum diode junction temperature given by the diode datasheet.

B. Current lead sizing

Current leads are designed to carry electrical current from room temperature to cryogenic temperature, while limiting the heat input inside the cryostat. For their sizing, we adopt here McFee's formula [22] that gives the minimum heat input $\dot{Q}_{L,min}$ as a function of the current lead nominal current I,

$$\dot{Q}_{L,min} = I\left[2\frac{\kappa}{\sigma}(T_H - T_L)\right]^{1/2} \qquad (2)$$

where I is the RMS or DC current [A], κ is the thermal conductivity [W/(K·m)], σ is the electrical conductivity [S/m], T_H is the temperature of the hot end [K], and T_L is the temperature of the cold end [K].

C. Cooling options

Assuming an operating temperature of 77 K, two cooling options are considered:

a) The cooling power is "free" and would be "lost" if not used. This is the case, for example, with future hydrogen-powered aircraft, where hydrogen is stored at cryogenic temperature before being reheated for use as fuel [23]. In this case, we only consider the power losses of each system element.

b) The cooling power needs to be produced using a cryocooler. In that case, it is necessary to consider the cryocooler efficiency η_c,

$$\eta_c = \frac{P_{cold}}{P_{c,e}} \qquad (3)$$

where P_{cold} is the cryocooler cold thermal power and $P_{c,e}$ is the electrical power consumed by the cryocooler. If we assume that the cooler efficiency is 20 % of the Carnot efficiency and since we operate at 77 K, then η_c is equal to 0.0714 [24]. This means that for each watt dissipated in the cryostat, the cooling system consumes 14 W.

D. Results

Table II summarizes the heat sink sizing for both topologies. For topology #T1, we choose the SK 412 50 SA AL heatsink from Fischer Elektronik. It is made of aluminum and its surface is black anodized. It has a height of 0.04 m and a width of 0.163 m. For topology #T2 where the diode rectifier is cooled by liquid nitrogen, the heat sink is much smaller. Indeed, we use a Fischer Elektronik's SK 85 AL heatsink, made of aluminum and black anodized surface with dimensions of 0.025 m in height and 0.75 m in width. This represents a reduction of 80% of the volume.

TABLE II
HEATSINK SIZING RESULTS

Symbol	Parameter	#T1	#T2
R_{HA}	Thermal resistance	1.048 K/W	4.523 K/W
H_{length}	Length	0.075 m	0.05 m
V_H	Volume	0.488 L	0.093 L
M_H	Mass	1.318 kg	0.253 kg

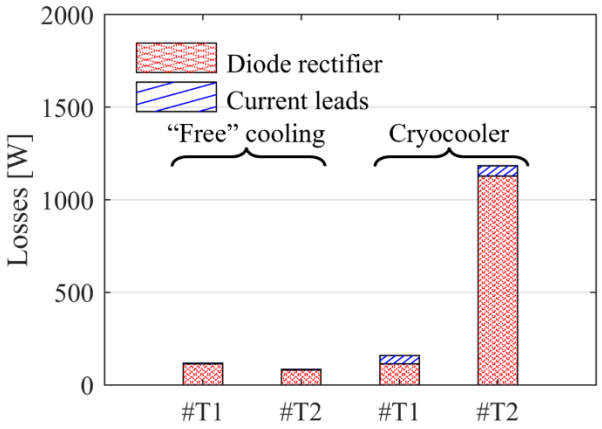

Fig. 8. Breakdown of the losses attributed to each element, for each topology and for both cooling options (for P_{dc} = 3.4 kW).

Fig. 8 compares the losses attributed to each element, omitting the losses of the load. It shows that the cryogenic converter is attractive when the cooling is "free". But if the cooling power has to be generated by a cryocooler, the diode losses inside the cryostat seriously penalize the cooling budget.

VI. CONCLUSION

In this study, several power diodes were characterized, showing different behavior when cooled to 77 K. We selected a diode with reduced conduction losses when used at cryogenic temperature to build a 3.4 kW 3-phase diode rectifier. The cryogenic converter operated as expected at both room and cryogenic temperatures. Operating the diode rectifier at liquid nitrogen temperature reduced losses by 28% and increased efficiency by 1%. We have also demonstrated that by using only the measured I-V characteristic of the diode at cryogenic temperature, it is possible to predict the performances of the cryogenic converter. Finally, we optimally sized both a conventional and a cryogenic diode rectifier for a given application. The results show that the cryogenic rectifier's heat sink is 80% lighter and more compact than that of the conventional rectifier. But, in terms of power consumption, the cryogenic converter only seems attractive when the cooling power is "free", as in future hydrogen-powered aircraft. In the future, it would be interesting to conduct a similar analysis while considering active components (e.g., MOSFETs) instead of diodes.

REFERENCES

[1] T. Winkler on behalf of the E. Consortium, “The EcoSwing Project,” IOP Conf. Ser. Mater. Sci. Eng., vol. 502, no. 1, art. 012004, Apr. 2019.

[2] G. Sarmiento et al., “Design, manufacturing and tests of first cryogen-free MgB2 prototype coils for offshore wind generators,” J. Phys. Conf. Ser., vol. 507, no. 3, art. 032041, May 2014.

[3] T.-K. Hoang, L. Quéval, C. Berriaud, L. Vido, “Design of a 20 MW fully superconducting wind turbine generator to minimize the levelized cost of energy,” *IEEE Transactions on Applied Superconductivity*, vol. 28, no. 4, pp. 1-4, Jun. 2018.

[4] L. B. S. Benitez, “E -Thrust, electrical distributed propulsion system concept for lower fuel consumption, fewer emissions and less noise,” [Online], 2015. Available: https://documents.pub/document/e-thrust-en-v13-final.html (accessed Feb. 14, 2023).

[5] J. L. Felder, “NASA N3-X with Turboelectric Distributed Propulsion,” [Online], 2014. Available: https://ntrs.nasa.gov/citations/20150002081 (accessed Feb. 13, 2023).

[6] “ASCEND - a first step towards cryogenic electric propulsion in aircraft,” [Online], 2021. Available: https://www.airbus.com/en/newsroom/stories/2021-03-cryogenics-and-superconductivity-for-aircraftexplained (accessed Feb. 13, 2023).

[7] R. R. Ward et al., "Power diodes for cryogenic operation," IEEE 34th Annual Conference on Power Electronics Specialist (PESC 03), vol.4, pp. 1891-1896, Acapulco, Mexico, 2003, doi: 10.1109/PESC.2003.1217741.

[8] H. Gui et al., "Review of Power Electronics Components at Cryogenic Temperatures," IEEE Transactions on Power Electronics, vol. 35, no. 5, pp. 5144-5156, May 2020, doi: 10.1109/TPEL.2019.2944781.

[9] H. Gui et al., "Characterization of 1.2 kV SiC Power MOSFETs at Cryogenic Temperatures," *IEEE Energy Conversion Congress and Exposition (ECCE)*, pp. 7010-7015, Portland, OR, USA, 2018, doi: 10.1109/ECCE.2018.8557442.

[10] B. Ozpineci and L. M. Tolbert, "Characterization of SiC Schottky diodes at different temperatures," *IEEE Power Electronics Letters*, vol. 1, no. 2, pp. 54-57, June 2003, doi: 10.1109/LPEL.2003.821026.

[11] A. Elwakeel, Z. Feng, N. McNeill, M. Zhang, B. Williams and W. Yuan, "Study of Power Devices for Use in Phase-Leg at Cryogenic Temperature," *IEEE Transactions on Applied Superconductivity*, vol. 31, no. 5, pp. 1-5, Art no. 5000205, Aug. 2021, doi: 10.1109/TASC.2021.3064544.

[12] “Diode BYT 60-400 datasheet” [Online]. Available: http://www.datasheet.hk/view_download.php?id=1504998&file=0254%5Cbyt60-400_148966.pdf (accessed Dec. 18, 2023).

[13] “Diode VS-HFA220FA120 datasheet, Vishay” [Online]. Available: https://www.vishay.com/docs/93636/vs-hfa220fa120.pdf (accessed Dec. 18, 2023).

[14] L. Quéval, D. Huchet, F. Trillaud, M. Kiuchi, T. Matsushita, “Test station for high temperature superconducting power cables,” *IEEE Transaction on Superconductivity*, in press, Dec. 2023.

[15] “Keithley 2182A nanovoltmeter datasheet” [Online]. Available: https://download.tek.com/datasheet/2182A-15912.pdf (accessed Dec. 18, 2023).

[16] “Current Probes A622 datasheet” [Online]. Available: https://www.tek.com/fr/datasheet/current-probes (accessed Dec. 18, 2023).

[17] “Differential voltage probe ST1000 datasheet” [Online]. Available: https://www.francaise-instrumentation.fr/media/productattachment/S/T/ST1000-2-sonde-differentielle-francaise-instrumentation-FR.pdf

[18] “PicoScope 4444” [Online]. Available: https://www.picotech.com/oscilloscope/4444/picoscope-4444-overview (accessed Dec. 18, 2023).

[19] “MATLAB, “Diode”, 2023” [Online]. Available: https://www.mathworks.com/help/sps/powersys/ref/diode.html (accessed Dec. 18, 2023).

[20] T. Halder, "Study of rectifier diode loss model of the Flyback converter," IEEE International Conference on Power Electronics, Drives and Energy Systems (PEDES), Bengaluru, India, 2012, doi: 10.1109/PEDES.2012.6484492.

[21] W. -Y. Choi, J. -M. Kwon, E. -H. Kim, J. -J. Lee, B. -H. Kwon, "Bridgeless Boost Rectifier With Low Conduction Losses and Reduced Diode Reverse-Recovery Problems," *IEEE Transactions on Industrial Electronics*, vol. 54, no. 2, April 2007, doi: 10.1109/TIE.2007.891991.

[22] R. McFee, “Optimum Input Leads for Cryogenic Apparatus,” *Rev. Sci. Instrum.*, vol. 30, no. 2, pp. 98–102, 1959.

[23] C. Hartmann, J. K. Nøland, R. Nilssen, R. Mellerud, “Dual Use of Liquid Hydrogen in a Next-Generation PEMFC Powered Regional Aircraft With Superconducting Propulsion,” *IEEE Trans. Transp. Electrification*, vol. 8, no. 4, pp. 4760–4778, Dec. 2022.

[24] D. Wikkerink, A. R. Mor, H. Polinder, R. Ross, “Converter Design for High Temperature Superconductive Degaussing Coils,” *IEEE Access*, vol. 10, pp. 128656–128663, Dec. 2022.